

# Carrier Concentration Dependent Resonance Frequency Shift in Metamaterial Loaded Semiconductor

Seiji Myoga<sup>1</sup>, Tomohiro Amemiya<sup>2</sup>, Atsushi Ishikawa<sup>3</sup>, Nobuhiko Nishiyama<sup>1</sup>, Takuo Tanaka<sup>3</sup> and Shigehisa Arai<sup>1,2</sup>

1) Dept. of Electrical and Electronic Engineering, Tokyo Institute of Technology, 2-12-1 O-okayama, Meguro-ku, Tokyo 152-8552, Japan

2) Quantum Nanoelectronics Research Center, Tokyo Institute of Technology, 2-12-1 O-okayama, Meguro-ku, Tokyo 152-8552, Japan

3) Metamaterials Laboratory, RIKEN, 2-1 Hirosawa, Wako, Saitama 351-0198, Japan

[myoga.s.ab@m.titech.ac.jp](mailto:myoga.s.ab@m.titech.ac.jp)

**Abstract**—We experimentally observed that the resonant frequency of the split ring resonator consisting of metal/semiconductor metamaterial varies with the carrier concentrations of the semiconductor layer

## I. INTRODUCTION

Using the permeability in photonic devices is an emerging challenge that can revolutionize the optical communication technology. One promising approach is to use the concept of *metamaterials* which are artificial materials designed to have permittivity and permeability values that are not possible in nature [1, 2].

When applying the concept of the metamaterials to actual applications, it is indispensable to control properties of the metamaterials for tuning electromagnetic responses (i.e., tunable metamaterials). A typical way to create the tunable metamaterials is to integrate a reconfigurable material into a metamaterial structure; thereby the active tuning is achieved by applying an external stimulus. GaAs-based modulators with split ring resonators (SRRs) [3] and metamaterial memories on a VO<sub>2</sub> film [4] are such device prototypes operating at a frequency of 1-10 THz.

Active tuning of the metamaterials at higher frequencies (e.g., optical frequency) is a promising challenge for future photonic devices combined with the metamaterials. In this paper, the effects of semiconductor carriers were explored to address the fundamental aspects of resonance tuning at around 60 THz (5- $\mu$ m wavelength), bringing optical frequencies into reach for controlling the permeability. We examined the response of near-infrared metamaterials consisting of SRRs fabricated on semiconductor GaInAs layers with different doping levels and investigated the possibility of resonant-frequency-shift controlled by changing carriers in semiconductors.

## II. FABRICATION AND MEASUREMENT RESULTS

Figure 1 shows the schematic structure of the device. The metamaterial samples were made on three different wafers. All wafers consist of a p-type doped GaInAs layer (150-nm thick) grown on a semi-insulating InP substrate by organo-metallic vapor phase epitaxy (OMVPE), which has the carrier concentration of  $1.9 \times 10^{18} \text{ cm}^{-3}$ ,  $1.2 \times 10^{19} \text{ cm}^{-3}$ , and  $2.6 \times 10^{19} \text{ cm}^{-3}$ , respectively. On the surface of the GaInAs layer, a SRR array consisting of 10-nm thick Ti and 40-nm thick Au was formed using electron-beam (EB) lithography and lift-off

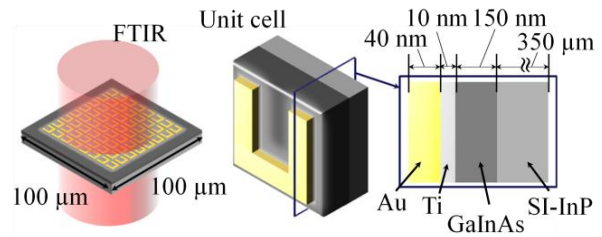


Fig. 1 The structure of the metamaterial sample consisting of a gold-based SRR array formed on p-GaInAs / semi-insulating-InP

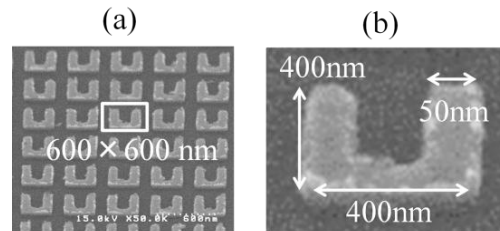


Fig. 2 (a) Scanning electron micrograph of a split-ring array with a total area of 100  $\mu\text{m}^2$ . (b) Enlarged oblique view of an individual split ring.

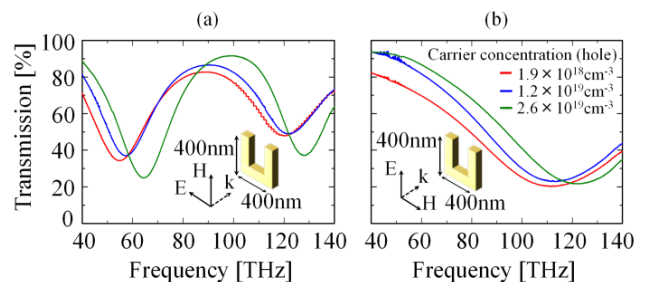


Fig. 3 Normal-incidence transmittance spectra for the (a) horizontal and (b) vertical polarizations, measured with different carrier concentrations of the GaInAs layer.

process. We used U-shaped SRRs with the dimensions given by the scanning electron micrographs shown in Fig. 2. In this study, SRRs of different sizes ranging from  $400 \times 400$  to  $1000 \times 1000$  nm (outer size of the square SRR ring) were prepared.

Figures 3 shows transmission spectra of the device with  $400 \times 400$ -nm SRRs, measured with a Fourier-transform infrared spectrometer. In this measurement, to clarify the effect of the interaction, we took the ratio of the transmission intensity of the experimental device (with SRRs) and that of the control device (without SRRs). For incident light with an electric field vector

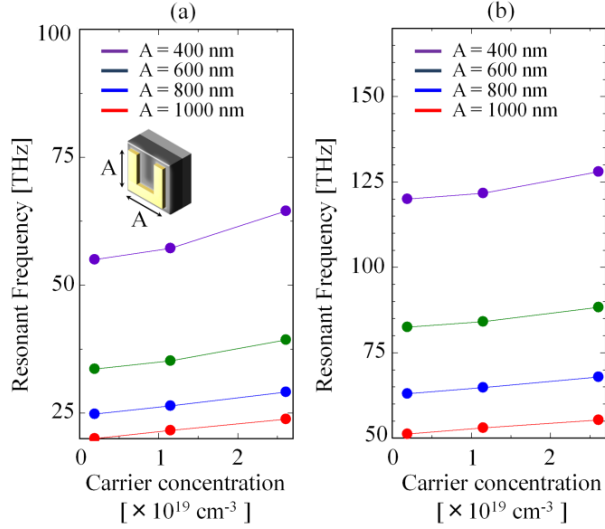


Fig. 4 (a) LC and (b) plasmonic resonance frequencies for devices with SRR size of  $400 \times 400$  nm,  $600 \times 600$  nm,  $800 \times 800$  nm, and  $1000 \times 1000$  nm as a function of carrier concentrations of the GaInAs layer, measured for the polarization perpendicular to the SRR gap.

perpendicular to the SRR gap, two distinct resonances were clearly visible (Fig. 3(a)). The resonance at the frequency of around 60-THz disappeared when the electric field vector was rotated by  $90^\circ$  (Fig. 3(b)), which was expected for the LC resonance. More importantly, a clear blue shift of the resonance was observed as the doping level of the GaInAs layer was increased.

Figure 4(a) and 4(b) show LC and plasmonic resonance frequencies of devices with different SRR sizes as a function of carrier concentration of the GaInAs layer, measured for the polarization perpendicular to the SRR gap. With increasing the SRR size, the resonance frequency decreased because of the enhancement of the loop inductance of the SRR ring. However, independent of the SRR size, the blue shifts of the resonance remained essentially unchanged. This clearly shows that the resonant frequency can be shifted by varying the carrier concentration.

### III. SIMULATION ANALYSIS

The resonance shift occurs because a resistance and a capacitance within the split gap are influenced by the carrier concentrations of the GaInAs layer. This can be explained by the free-carrier absorption model [5].

We confirmed the resonant frequency shift of the device through a simulation using a 3-dimensional full-wave solver based on the finite element method. From the free-carrier absorption model, the permittivity  $\varepsilon$  and electric conductivity  $\sigma$  of the semiconductor GaInAs layer are given by

$$\varepsilon(\omega, N) = \varepsilon_0 \varepsilon_r \left\{ 1 - \frac{[\omega_p(N)\tau(N)]^2}{1 + [\omega\tau(N)]^2} \right\}, \quad (1)$$

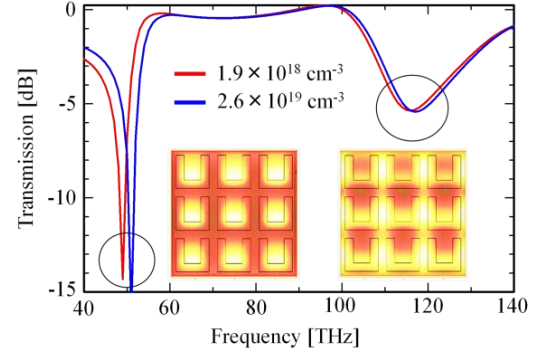


Fig. 5 Calculated transmission spectra, corresponding to the experiments shown in Fig. 3(a). Insets visualize the distribution of magnetic field in the SRR array at minimum-transmission frequencies.

$$\sigma(\omega, N) = \frac{\sigma_0(N)}{1 + [\omega\tau(N)]^2}, \quad (2)$$

where  $\omega$  is the angular frequency of light,  $N$  is the carrier concentration,  $\varepsilon_0$  and  $\varepsilon_r$  are the vacuum permittivity and the static permittivity, respectively,  $\omega_p(N)$  is the plasma frequency,  $\tau(N)$  is the mean free time,  $\sigma_0(\omega)$  is the static electric conductivity. In this simulation, the hole mobility was set to 111 cm/Vs for  $N=1.9 \times 10^{18}$  cm $^{-3}$ , 60 cm/Vs for  $N=2.6 \times 10^{19}$  cm $^{-3}$ . In addition, a conductivity of the metal Ti/Au was assumed to be defined by the Drude model.

Figure 5 shows the simulated transmission spectra, corresponding to the experiments shown in Fig. 3(a). The insets in Fig. 5 visualize the distribution of electric field in a SRR at minimum-transmission frequencies. This distribution shows that, at 50 THz, the magnetic response of the SRR array is dominant in our device. As shown in Fig. 5, resonant frequency shifted to a shorter wavelength side for larger carrier concentration in the GaInAs layer and such a trend agreed with the experimental results.

In summary, we demonstrated that the resonant frequency of the near-infrared metamaterial was controlled by changing the carrier concentrations of the GaInAs layer on which split ring resonators were fabricated.

### ACKNOWLEDGEMENT

This research was financially supported by the Ministry of Education, Culture, Sports, Science and Technology (MEXT), Japan and the Japan Society for the Promotion of Science (JSPS) under Grants-in-Aid for Scientific Research (#19002009, #22360138, #21226010, #23760305).

### REFERENCES

- [1] H. J. Lezec, J. A. Dionne, and H. A. Atwater, "Negative refraction at visible frequencies," *Science*, vol. 316, no. 5823, pp. 430–432, 2007.
- [2] H. Chen, "Metamaterials: constitutive parameters, performance, and chemical methods for realization," *J. Mater. Chem.*, vol. 21, 6452, 2011.
- [3] H. T. Chen, *et al.*, "Active terahertz metamaterial devices," *Nature*, vol. 444, no. 7119, pp. 597–600, 2006.
- [4] T. Driscoll, *et al.*, "Memory Metamaterials," *Science* vol. 325, no. 5947, pp. 1518–1521, 2009.
- [5] M. Shirao, *et al.*, "Preliminary Experiment on Direct Media Conversion from a 1.55  $\mu$ m Optical Signal to a Sub-Terahertz Wave Signal Using Photon-Generated Free Carriers," *Jpn. J. Appl. Phys.*, vol. 48, 2009.